

9.3 Spectrum Analysis for Repair

As discussed in Section 9.2, the flight-by-flight crack growth rate behavior for many structural loading conditions can be defined using a power law that relates crack growth rate to a characteristic stress-intensity factor, i.e.

$$\frac{da}{dF} = C\bar{K}^P \quad (9.3.1)$$

An example analysis is conducted using three transport wing stress histories to illustrate how such equations can be generated. Subsequent to the generation of the flight-by-flight crack growth rate equations, additional analysis is conducted to evaluate the effects stress level and structural location on the use of these equations for the structural repairs.

9.3.1 Definition of Stress Histories

The transport stress histories utilized for this example were developed during a force management update and represent the expected behavior at three separate locations on the lower wing surface. The force management update involved a complete durability and damage tolerant analysis of the airframe, as well as reassessment of past and future usage of the aircraft force. Stress histories were generated for durability and damage tolerant studies at those structural locations identified as potentially critical to the continuing safe operation of the force.

The lower wing stress histories chosen for this example analysis represent locations in the center wing (BL 70), in the inner wing (WS 733) and the outer wing. All three stress histories were developed assuming the same operation (mission mix) history. The operational history was considered to be represented by a block of 100 flights with a defined mission order. Eight (8) separate missions were identified as representative of service operations. Each mission in the 100-flight block averaged 4.8 hours per flight.

The 100-flight block of ordered missions repeated until the service life of 40,000 flight hours was exceeded; thus, more than 83 applications of the repeating 100-flight blocks were required to define a lifetime of operation. The mission order for the eight representative missions is defined by [Table 9.3.1](#). For comparison purposes, [Figure 9.3.1](#) presents the stress histories for mission one at three locations. The stress histories for the other seven missions could be defined in a similar manner.

Table 9.3.1. Mission Ordering for Transport Flight-by-Flight Spectrum

Order Per 20 Flight Group	Flights 1-20	Flights 21-40	Flights 41-60	Flights 61-80	Flights 80-100
1	4	6	7	6	5
2	1	7	7	1	4
3	1	7		6	1
6	7	2	3	7	1
5	6	1	6	6	1
6	4	4	2	5	8
7	5	3	6	3	2
8	2	8	7	7	3
9	5	5	3	4	8
10	8	4	8	2	6
11	2	3	8	3	7
12	8	1	7	6	5
13	2	6	3	5	6
14	7	6	1	6	6
15	1	3	8	7	6
16	6	8	5	7	5
17	7	6	7	6	1
18	7	1	6	2	5
19	2	2	2	5	4
20	7	4	4	4	7

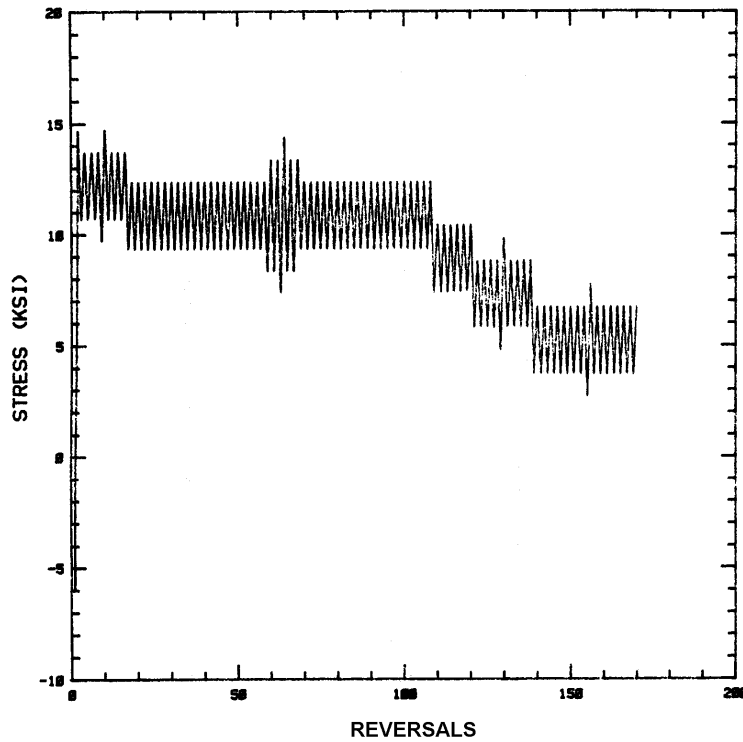


Figure 9.3.1a. Center Wing Stress History for Mission 1

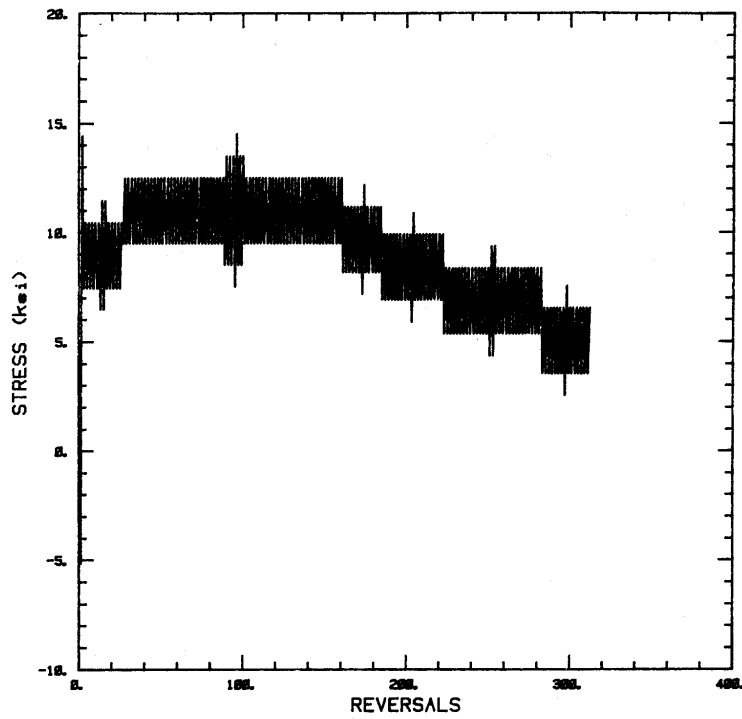


Figure 9.3.1b. Inner Wing Stress History for Mission 1

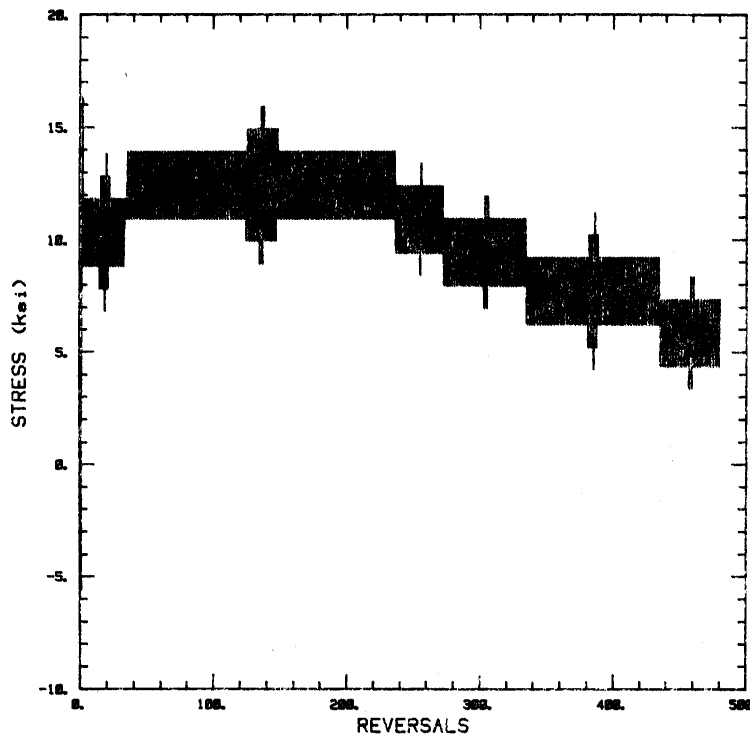


Figure 9.3.1c. Outer Wing Stress History for Mission 1

The stress history for each location is now defined except for the infrequently occurring maximum stresses. The infrequently occurring stresses in each mission were inserted into the history on a periodic basis as a replacement for the first maximum stress in the mission. The period of occurrence of these replacement load events was during the tenth, the one-hundredth, and the two-hundredth repeat occurrence of any of the individual eight missions. The replacement maximum stresses for mission 1 for the three locations are listed in [Table 9.3.2](#). Each mission had a similar set of replacement stresses.

Table 9.3.2. Replacement Stresses for Mission 1 for the Three Wing Locations

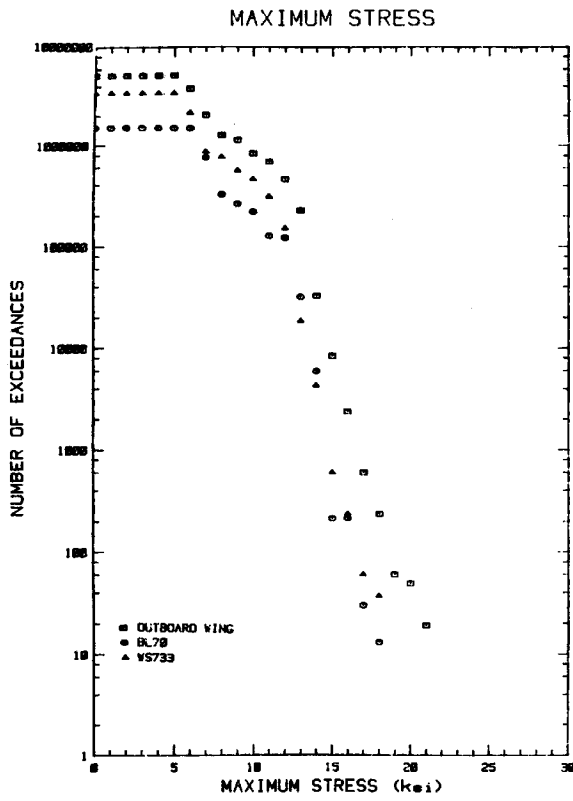
Occurrence Frequency (per no. of mission repeats)	Center Wing (BL-70) Location (ksi)	Inner Wing (WS-733) Location (ksi)	Outer Wing Location (ksi)
1/1	14.64	14.43	16.34
1/10	16.16	16.16	18.36
1/100	17.96	17.96	20.79
1/200	18.6	18.60	21.56

9.3.2 Spectra Descriptions

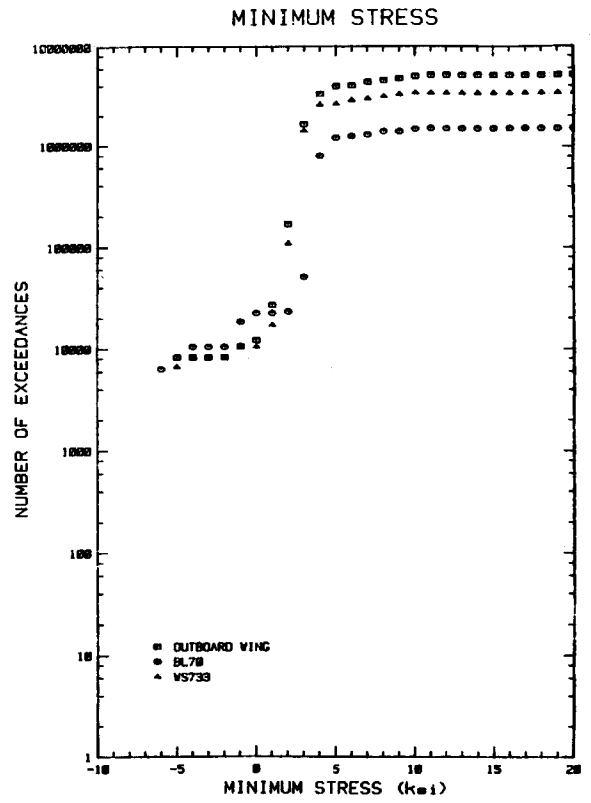
The stress history uniquely defines the sequence and magnitude of the individual stress events applied at a specific location. While this information is essential for conducting a cycle-by-cycle crack growth analysis that accounts for load interaction, it is both difficult to use and interpret without computer programs that perform such analyses. One of the side benefits associated with describing flight-by-flight crack growth rates as a function of a characteristic stress-intensity factor is that one is forced into presenting stress history information simply. This subsection addresses two such schemes – the exceedance curve and an RMS characterization.

9.3.2.1 Exceedance Curve Descriptions

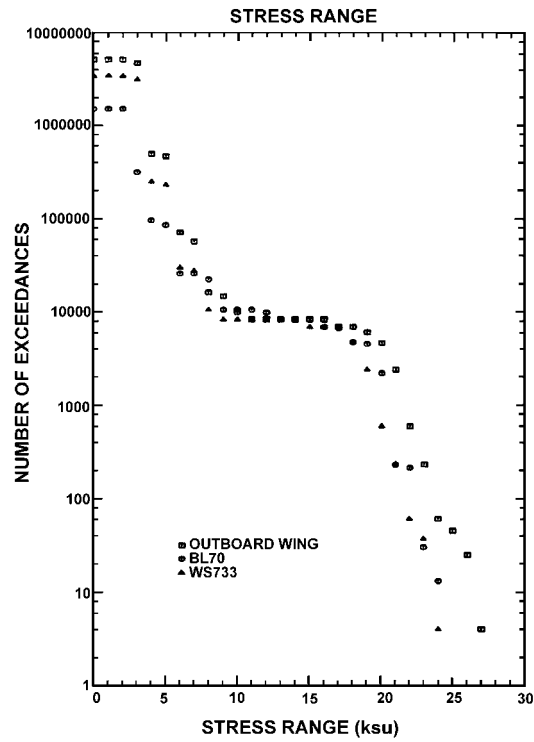
One normally generates a stress history for a given mission based upon exceedance information; however, the starting exceedance information is typically based in operational parameters, e.g. n_z , airspeed, weight, altitude, etc. for given mission functions. After a stress history has been generated for a collection of missions, it is recommended that stress exceedance curves be generated for the maximum stress, the minimum stress, and the positive (load-increasing) stress range associated with all stress events. The exceedance curves for the maximum, minimum, and range of the individual stress events in the three wing stress histories are presented in [Figure 9.3.2](#).



(a) Maximum Stress Exceedance



(b) Minimum Stress Exceedance



(c) Stress Range Exceedance

Figure 9.3.2. Exceedance Curves for the Three Transport Wing Stress Histories

The exceedance curves for each stress event characteristic are noted (from [Figure 9.3.2](#)) to be similar in shape but somewhat displaced relative to number of exceedances. The behavior observed might have been expected since all three locations are experiencing the same operational history. Both the minimum stress and stress range exceedance curves indicate a plateau around 8300 exceedances, which is the dividing line between once per flight occurrences and those that occur more frequently. Thus, because we are dealing with a transport aircraft, it can be noted that the once per flight ground-air-ground (GAG) cycle has a stress range typically larger than 16 ksi, while the gust/maneuver cycles have stress ranges less than 8 ksi.

In anticipating the level of damage that a stress history might generate, the exceedance curve becomes a useful tool. The highest stresses (all events) are noted to be present in the outboard wing (followed by the inner wing and then center wing). Also, for a given magnitude of any stress characteristic, the number of exceedances are the highest for the outboard wing location (followed by the inner wing and center wing). The implication is that, on a per flight basis, more damage is generated at the outer wing location than at the other two locations, all other things being equal (structural geometry, material, crack geometry, etc.).

The shape of the exceedance curve can also be used to determine if the stress history might be expected to introduce major perturbations in the crack growth behavior. If the exceedance curve associated with the maximum stress characteristic is relatively continuous from the infrequency of the once-per-flight event, then the flight-by-flight crack growth rate curve would also be expected to be relatively continuous. Except for the outboard wing location curve between 40-60 exceedances, [Figure 9.3.2a](#) shows that the maximum stress exceedance curves are relatively continuous. It is therefore expected that the flight-by-flight crack growth rate curves for the three wing histories will be relatively continuous (not show major effects of retardation).

9.3.2.2 RMS Descriptions

The presentation of complicated variable amplitude stress histories can be simplified by defining average or RMS values of the stress event characteristics, i.e. the maximum stresses and positive stress ranges of the history. The difference between the average value and the RMS value of a given characteristic is normally not more than 3 percent when one is considering stress histories with more than 1000 stress events. For average stress analysis, one uses

$$\sigma_{mean} = \sum_{i=1}^N \left(\frac{\sigma_i}{N} \right) \quad (9.3.2)$$

while for RMS analysis, one uses

$$\sigma_{RMS} = \left[\sum_{i=1}^N \frac{\sigma_i^2}{N} \right]^{\frac{1}{2}} \quad (9.3.3)$$

where σ_i is the characteristic (maximum stress or stress range) for the i^{th} stress event and N is the total number of stress events.

Similar analysis schemes have also been employed where the slope (p) of the crack growth rate power law expression (Equation 9.3.1) is used to calculate a representative stress, i.e.

$$\sigma_{REP} = \left[\sum_{i=1}^N \sigma_i^{\frac{p}{N}} \right]^{\frac{1}{p}} \quad (9.3.4)$$

Experience has shown that such schemes (Equation 9.3.4) are not appreciably of more value than the average or RMS determined characteristics.

The RMS equation (Equation 9.3.3) was applied to the three transport wing stress histories to obtain RMS values for the maximum stress and stress range. The results are summarized in [Table 9.3.3](#).

Table 9.3.3. Per Cycle Root Mean Square (RMS) Representative Stress Values for the Three Wing Stress Histories

Stress History	Maximum Stress (ksi)	Stress Range (ksi)	Cycles per 100 Flights
Center Wing (BL-70)	8.00	3.52	18268
Inner Wing (WS-733)	7.24	3.33	41174
Outer Wing	8.01	3.38	62562

Based on the RMS analyses presented in [Table 9.3.3](#), it appears as if the three stress histories are quite similar on a per cycle basis (the stress ranges are within five (5) percent, and the maximum stresses are within ten (10) percent). Based on a constant amplitude analysis of these stress conditions, the damage per cycle would be expected also to be similar. From [Table 9.3.3](#), one can note the number of cycles applied per 100 flight block differs substantially from stress history to stress history. If the RMS stresses are similar and the number of stresses per flight differ, then one would expect that the damage per flight would favor the stress history with the most stress events per flight.

One of the reasons that the RMS representative stresses can not be blindly used in a constant amplitude equation to accurately estimate crack growth behavior is because the damage is a non-linear function of the different events in the history. The analyst must understand where the damage is coming from and isolate on those events. For example, a transport wing stress history generates damage as a result of both GAG cycle loading and gust/maneuver cycle loading. A second analysis was therefore conducted on the three wing histories to obtain per flight characteristics for the GAG and gust/maneuver cycles. This analysis is presented in [Table 9.3.4](#).

Table 9.3.4. Per Flight Root Mean Square Representative Stress Values for the Three Wing Stress Histories

Stress History	GAG Max Stress (ksi)	GAG Min Stress (ksi)	Gust/Manu. Max Stress (ksi)	Gust/Manu. Stress Range (ksi)	Number of Gust/Maneuver Cycles
Center Wing (BL-70)	12.23	18.64	7.97	3.35	182
Inner Wing (WS-733)	13.14	18.13	7.21	3.31	411
Outer Wing	14.73	20.01	7.99	3.29	625

Relative to the per flight RMS representative stress values for GAG and gust/maneuver cycles, the three stress histories are shown to be relatively similar. The magnitude of the GAG cycle appears to be increasing as the location moves outboard; this would indicate that the GAG cycle causes more damage per flight in the outboard wing than at the inner and center wing locations. We note that the largest number of gust/maneuver cycles occur at the outer wing location and this would also favor more damage per flight (due to gust/maneuver cycles) than the other two locations.

9.3.3 Crack Growth Analysis

To obtain a flight-by-flight crack growth rate equation (Equation 9.3.1), it is necessary to have either a crack growth life curve or the capability for generating such a curve. As described in Section 9.2, once a flight-by-flight crack growth life curve exists, it can be differentiated to obtain crack growth rates.

The simplest manner for differentiating a curve is by using the secant method, i.e.

$$\frac{da}{dF} = \frac{a_2 - a_1}{F_2 - F_1} \quad (9.3.5)$$

where (a_1, F_1) and (a_2, F_2) represent two different points on the crack growth life, crack length (a) versus flights (F) curve. The derivative is considered to be the slope of the curve at the mean crack length of the two points, i.e.

$$a_{mean} = \frac{1}{2}(a_1 + a_2) \quad (9.3.6)$$

The mean crack length provides the ability to calculate the stress-intensity factor coefficient (K/σ) for the geometry associated with the crack growth life curve. To describe the crack growth rate as a function of stress-intensity factor, it is necessary to have either a formula or graph that relates stress-intensity factor to crack length for a known external loading condition. For example, if the stress-intensity factor is related to gross stress conditions (σ_{gross}) by the formula

$$K = \sigma_{gross} \cdot \beta \sqrt{\pi a} \quad (9.3.7)$$

Then the stress-intensity factor coefficient is

$$\frac{K}{\sigma_{gross}} = \beta\sqrt{\pi a} \quad (9.3.8)$$

and Equation 9.3.8 is evaluated for $a = a_{mean}$ (Equation 9.3.6). Note that β is typically a function of crack length.

9.3.3.1 Generation of Crack Growth Curves

Crack growth life curves were generated for the three transport wing stress histories using a crack growth analysis computer code. The material chosen for the study was a 7075-T651 aluminum alloy; the associated constant amplitude crack growth rate curve was

$$\frac{da}{dN} = \frac{5 \times 10^{-7} \left(K_{max} (1 - R)^{\frac{2}{3}} \right)^3}{K_C - K_{max}} \quad (9.3.9)$$

with $K_C = 68$ ksi \sqrt{in} and $R = -0.12$. The Willenborg-Chang retardation model embedded within the software was used to account for load-interaction effects. These modeling choices affect the absolute accuracy of the crack growth predictions but not the implications of the analysis which are presented in a relative sense.

Rather than dealing directly with the actual structural geometries for the three wing locations, it was decided that the crack growth analysis would be applied for a common geometry for all three stress histories. This choice does not affect the crack growth rate analysis as will be further discussed below. The choice of common geometry for all three stress histories makes it possible to evaluate the relative effects of per flight and per cycle damage for the analyses. It was decided also to choose a simple geometry of a four (4) inch wide center cracked panel, giving a stress-intensity factor coefficient of

$$\frac{K}{\sigma} = \left(\pi a \cdot \sec \frac{\pi a}{W} \right)^{\frac{1}{2}} \quad (9.3.10)$$

The initial and final crack length chosen for the configuration were 0.11 and 1.25 inch, respectively. [Figure 9.3.3](#) summarizes the common configuration employed in this analytical study.

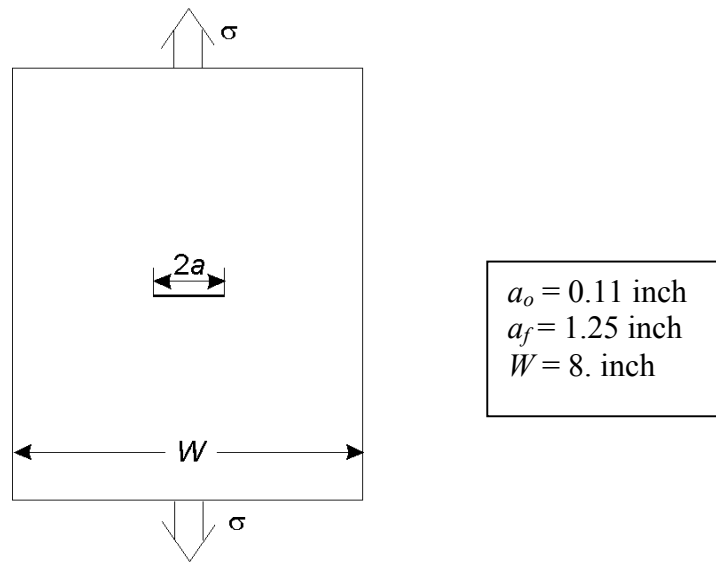
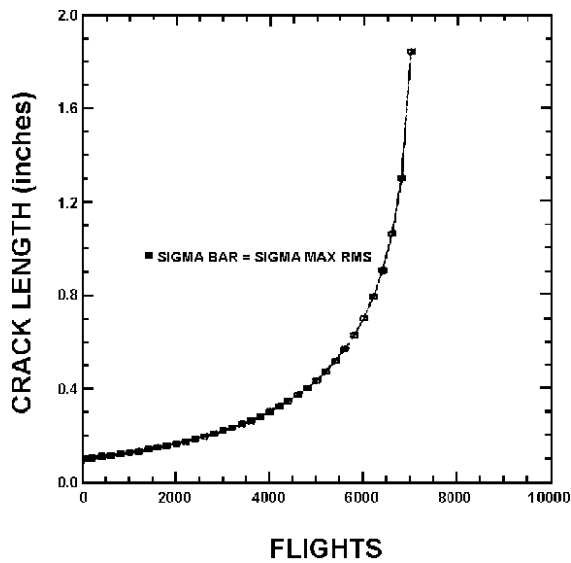


Figure 9.3.3. Common Geometry Used to Evaluate Stress History Effect on Crack Growth Behavior

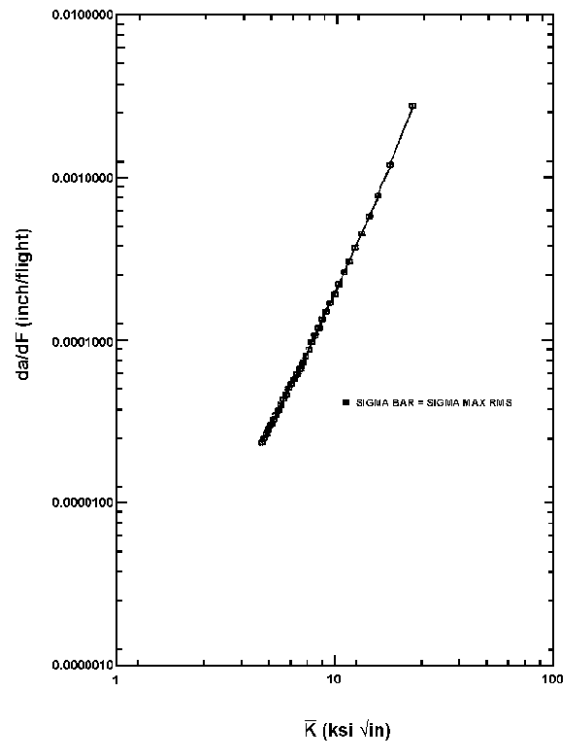
[Figure 9.3.4](#) presents both the crack growth life curve and its crack growth rate counterpart for the center wing stress history. The crack growth rate curve was generated by forming the secant defined slope for consecutive points on the life curve and relating this slope to the stress-intensity factor calculated using the mean crack length and the RMS maximum stress values (given in [Table 9.3.3](#)). The stress-intensity factor in [Figure 9.3.4](#) is given by

$$K = (\sigma_{\max})_{RMS} \cdot \left(\frac{K}{\sigma} \right) \quad (9.3.11)$$

where $(\sigma_{\max})_{RMS} = 8.0$ ksi, and (K/σ) is given by Equation 9.3.10. The curve through the center of the points in [Figure 9.3.4](#) is the mean trend curve that connects all the points.



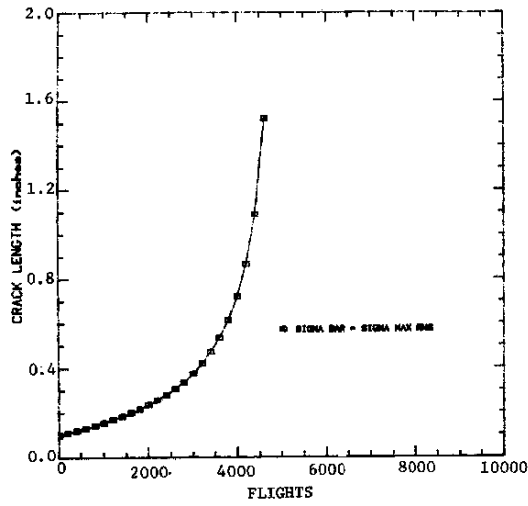
(a) Crack Growth Life Behavior



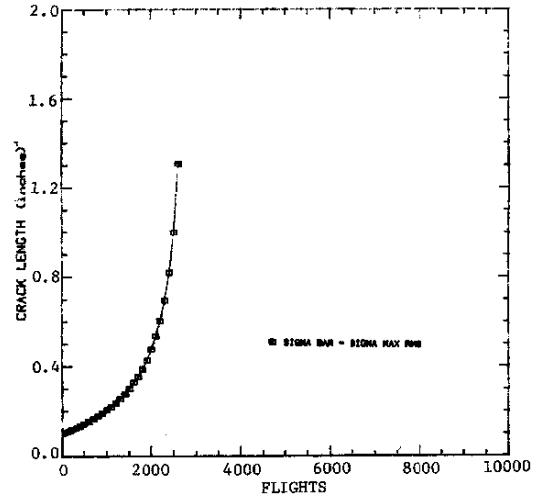
(b) Crack Growth Rate Behavior

Figure 9.3.4. Crack Growth Behavior for the Center Wing Location

[Figure 9.3.5](#) presents the crack growth life curves generated for the other two wing locations, again using the computer code. [Figure 9.3.6](#) summarizes the crack growth rate behavior associated with all three stress histories. The inner and outboard wing crack growth rate data points were also generated by the secant method of analysis. The RMS maximum stresses used for the stress multiplier in Equation 9.3.11 were 7.24 and 8.01 ksi for the inner wing and the outer wing location, respectively.



(a) Inner Wing



(b) Outer Wing

Figure 9.3.5. Flight-by-Flight Crack Growth Life Behavior for Inner Wing (WS-733) and Outboard Wing Stress Histories

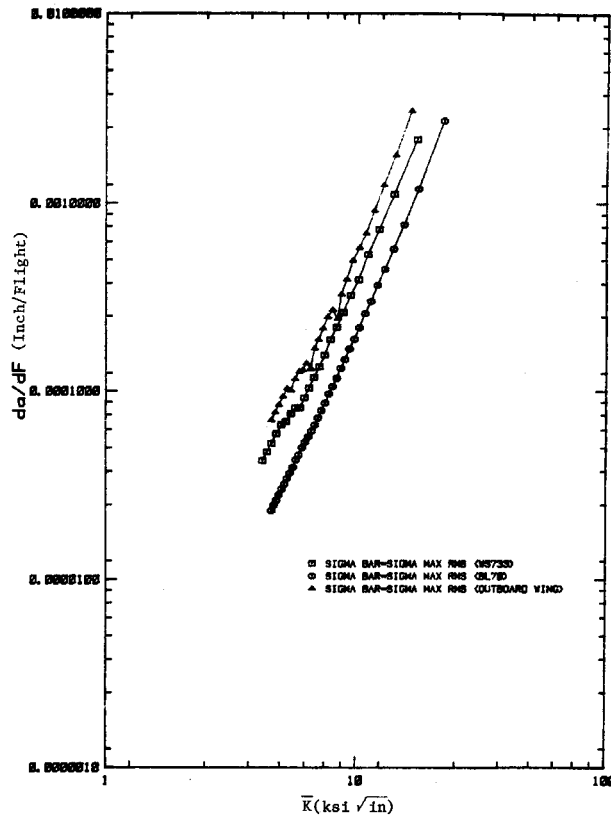


Figure 9.3.6. Flight-by-Flight Fatigue Crack Growth Rate Behavior for Three Transport Wing Histories

9.3.3.2 Analysis of Observed Behavior

A number of observations can be made from the data presented in [Figures 9.3.4](#) through [9.3.6](#). First, the life is shortest and the rates are fastest for the outer wing stress history; this stress history is the most damaging from a crack growth point of view. The next most damaging history is the inner wing stress history; the least damaging history is associated with the center wing location. Second, the three crack growth rate curves appear to be almost parallel and relatively continuous throughout the range shown. There are discontinuities in the outer and inner wing curves which tend to locally depress the rate curves. These discontinuities are not severe and are associated with the exceptionally high but frequently occurring maximum stress events in the stress history.

As a result of the relatively continuous nature of the crack growth rate curves, least square procedures were applied to the data in [Figure 9.3.6](#) in order to generate the constants in Equation 9.3.1. These constants are presented in [Table 9.3.5](#) along with another set of constants derived using graphical procedures and the assumption that the crack growth rate curves were parallel. [Figure 9.3.7](#) illustrates the degree of fit achieved by the curve established using least squares procedures for the outer wing data. The least squares determined power law curve is seen to adequately describe the outer wing data. The other two least squares power law curves provided similarly adequate descriptions of their respective crack growth rate data.

Table 9.3.5. Constants C and p for Equation 9.3.1

Stress History	Least Squares Method		Graphical Method	
	C	p	C	p
Center Wing (BL-70)	2.54×10^{-7}	2.93	3.35×10^{-7}	2.89
Inner Wing (WS-733)	7.29×10^{-7}	2.73	5.10×10^{-7}	2.89
Outer Wing	7.74×10^{-7}	2.86	9.05×10^{-7}	2.89

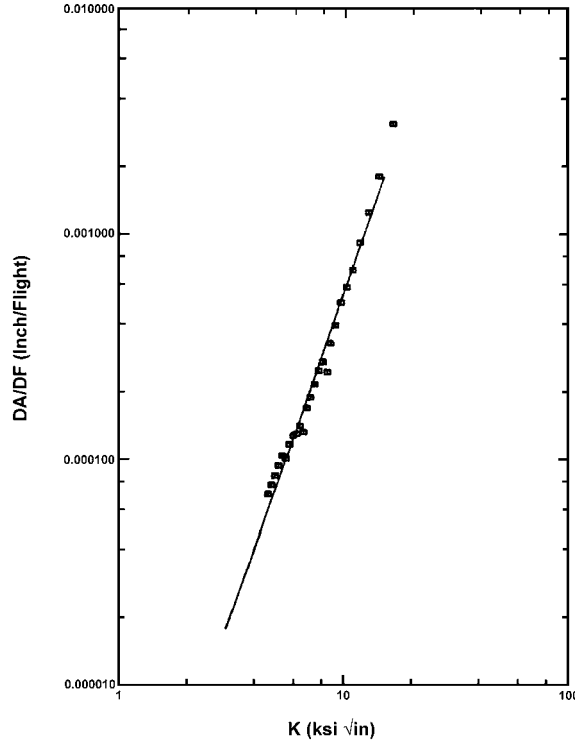


Figure 9.3.7. Comparison Between Outer Wing Data and the Least Squares Determined Curve

A second crack growth life analysis was conducted using the three transport wing stress histories scaled to a lower stress level; all stress events in the three histories were scaled to 0.903 of their original level (both tensile and compressive levels were scaled equally). The same computer software was employed for this second analysis, and all geometry and material properties were kept the same. The stress history mission mix and order (stress sequence) were the same as described in [subsection 9.3.1](#). As expected, longer crack growth lives were associated with the lower stress magnitude stress histories. [Table 9.3.6](#) summarizes the life predictions required to grow the crack between the previously defined limits of $2a_0 = 0.22$ inch and $2a_f = 1.60$ inch.

Table 9.3.6. Effect of Stress Magnification Factor on Crack Growth Lives (L)
Calculated for a Center Crack ($2a$) Growing Between 0.22 and 1.60 inch

Stress History	Lives for Two Stress Magnification Factor Values		Life Ratio $L_{0.903}/L_1$
	L_1 (Flights)	$L_{0.903}$ (Flights)	
Center Wing (BL-70)	6220	8300	1.33
Inner Wing (WS-733)	4115	5345	1.30
Outer Wing	2385	3117	1.31

9.3.3.3 Interpretation and Use of Crack Growth Rate Curves

It can be noted from [Table 9.3.6](#) that the ratios of crack growth lives for the two stress magnification factors are nearly the same (within 2 percent) for the three stress histories. The reason for this happening can be justified on the basis of the crack growth rate behavior. Consider [Figure 9.3.8](#) where both the crack growth life and crack growth rate behavior associated with the scaled inner wing stress histories are described. [Figure 9.3.8](#) shows that while the life behavior is different, the crack growth rate behavior can be described by a common curve. If the common crack growth rate curve is a power law equation (Equation 9.3.1) then its integral form, i.e.

$$F = \int_{a_0}^{a_f} \frac{da}{C\bar{K}^p} \quad (9.3.12)$$

can be written, using Equations 9.3.10 and 9.3.11, as

$$F = \frac{1}{C(\sigma_{max_{RMS}} \sqrt{\pi})^p} \cdot \int_{a_0}^{a_f} \frac{da}{\left(a \cdot sec \frac{\pi a}{W}\right)^{p/2}} \quad (9.3.13)$$

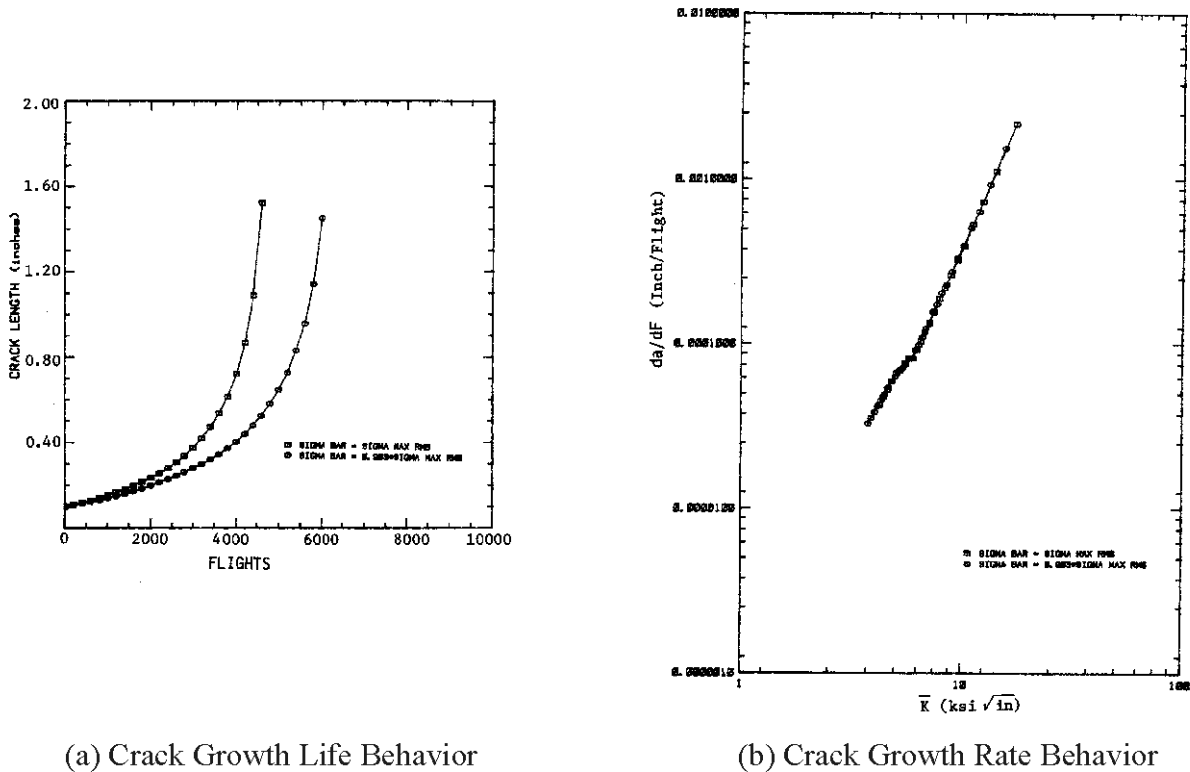


Figure 9.3.8. Flight-by-Flight Crack Growth Behavior Exhibited for the Inner Wing (WS733) Stress History Scaled to two Different Stress Levels

If all the stresses in a stress history are scaled, then the σ_{max} characterizing stress will be scaled by the same factor. So, if the crack growth interval remains the same, the life ratio ($L_{0.903} / L_1$ where $L_1 = F$ and $L_{0.903} = F$ with lower stress) is given by:

$$\frac{L_{0.903}}{L_1} = \frac{(\sigma_{\max_{RMS}})^p}{(0.903 \cdot \sigma_{\max_{RMS}})^p} = (0.903)^{-p} \quad (9.3.14)$$

Since all other factors in Equation 9.3.13 are constant, note that the integral is only a function of geometry and once the geometry is defined the stress level does not influence its value.

Using Equation 9.3.14 and the power law exponents given in [Table 9.3.5](#), the life ratio for the scaled stress histories is noted to vary between 1.32 and 1.35 (lowest value of exponent yield lowest life ratio). The life ratio estimate based on the crack growth rate power law exponent is noted to closely approximate the life ratios given in [Table 9.3.6](#). Thus, if one can obtain an estimate of the crack growth rate power law exponent, then one can closely approximate the effect of stress scaling on the crack growth life behavior. Section 9.4 provides additional information on the use of this analysis approach for estimating the lives of structural repairs.

Independent of the above remarks, Equation 9.3.12 has an important application for directly estimating the structural life of cracked components. As an example of its use for conducting such analysis, we compared the results of the computer analysis with life estimates made using the data presented in [Table 9.3.5](#) and Equation 9.3.13. These results are presented in [Table 9.3.7](#), where it is seen that the power law life prediction ratios, which are conservative relative to the least squares procedure, result in estimates which more closely approximate the estimates for all three stress histories.

Table 9.3.7. Ratio of Power Law Life Predictions (L_{PL}) to Life Predictions (L_{CG})
(Ratio > 1, Unconservative)

Stress History	Stress Magnitude Factor =1			Stress Magnitude Factor =0.903		
	Flights	L_{PL}/L_{CG}		Flights	L_{PL}/L_{CG}	
		Least Squares	Graphical		Least Squares	Graphical
Center Wing (BL- 70)	6220	0.961	0.789	8300	0.773	0.632
Inner Wing (WS-733)	4115	0.752	0.769	5345	0.772	0.803
Outer Wing	2385	0.945	0.761	3117	0.977	0.790

Because the least squares determined coefficients are insensitive to the accuracy with which the crack growth rate data are described, it is suggested that the analyst comparatively review the least squares results in a graphical format such as [Figure 9.3.7](#). One reason for choosing the

graphical method is to emphasize the (log-log) lower portion of the crack growth rate behavior. (The least squares procedure results in a "best" fit to all the data).

When flight-by-flight crack growth rate behavior is shown to be independent of stress scaling effects, the behavior will also be independent of the geometry used to collect the crack growth life data. This has been shown for a number of aircraft stress histories similar to those analyzed in this section.

One cautionary remark must be made relative to geometrical effects - if one reduces crack growth life data using a stress-intensity factor which is substantially in error of the actual stress-intensity factor for the geometry, then the transference of the crack growth rate data from one geometry to another will not be possible. In other words, take care in reducing crack growth life data from structural geometries where the stress-intensity factor is not well defined.

9.3.3.4 Analysis for Multiple Stress Histories

Air Logistics Center (ALC) engineers typically need to analyze structural locations within a component for which no stress history is available. Frequently, a stress analysis of these structural locations must be performed based on a strength of materials approach. One question asked repeatedly is: What is available that facilitates conducting a simple crack growth life analysis of these structural locations?

One method that has potential for a relatively large component is a wide area crack growth rate equation that describes the rate of damage growth within the area identified. This section provides an example of how a wide area crack growth rate equation might be generated and then utilized. The three transport wing stress histories provide the basis for this example.

To develop a wide area crack growth rate equation it is necessary to have crack growth life behavior described at a number of locations within the area of application. The mission mix and stress sequencing must be the same at all locations considered. It is anticipated that crack growth lives might be generated for ten or more locations experiencing loading conditions which produce similar contributions of damage. For the example, only three locations were analyzed for the entire wing; however, the approach and interpretation of results would be similar independent of the component and numbers of location.

As was shown in [Figure 9.3.6](#), the flight-by-flight crack growth rate behavior associated with the three stress histories was different; the rate behavior of each was seen to be relatively continuous and parallel to the others. To obtain a wide area crack growth rate equation, the analyst must find a method for collapsing the rate curves into one master curve. This collapsing can only be accomplished (with confidence) if the analyst understands the relationship between the damage generation process and the stress events in the history. The damage may be generated primarily either by the gust/maneuver cycles or by the GAG cycles.

[Figure 9.3.6](#) shows that the crack growth rates are ordered for the three histories according to the number of gust/maneuver cycles that occur per flight. The data in [Figure 9.3.6](#) were therefore converted to a crack growth rate per cycle basis and replotted. [Figure 9.3.9](#) describes the result of this scaling of crack growth rates. As is shown by [Figure 9.3.9](#), the crack growth rates are found to collapse to tight scatter band with the inner wing location behavior forming the upper curve on the band.

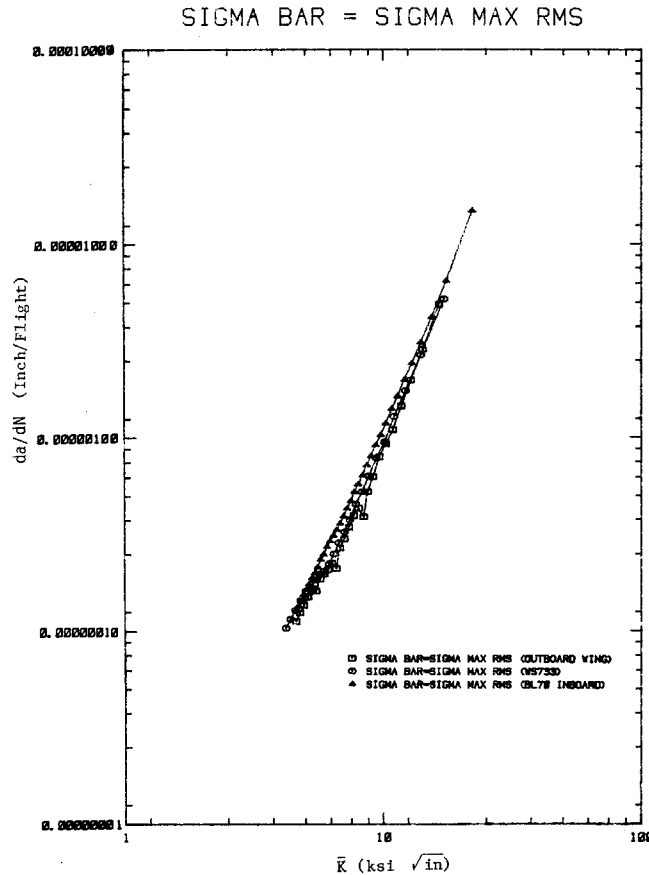


Figure 9.3.9. Cyclic Crack Growth Rate Behavior for Three Transport Wing Stress Histories

$$\bar{K} = \sigma_{\max_{RMS}} \cdot (K / \sigma)$$

The collapsing of crack growth rate data observed in [Figure 9.3.9](#) does not always occur when the $\sigma_{\max(RMS)}$ parameter is used as the stress history characterizing parameters. If the analyst uses a characterizing parameter that does not describe those events that create damage, one would not expect the crack growth rate data to collapse. Another good characterizing stress parameter for the three transport wing stress histories is the root mean square (RMS) stress range ($\Delta\sigma_{RMS}$). [Figure 9.3.10](#) describes the cycle-by-cycle crack growth rate behavior for the three stress histories where the characterizing stress-intensity factor (K) was calculated using

$$\bar{K} = \Delta\sigma_{RMS} \left(\frac{K}{\sigma} \right) \tag{9.3.15}$$

As [Figure 9.3.10](#) illustrates, the characterizing stress-intensity factor given by Equation 9.3.14 also collapses the rate data. Additional choices of the characterizing stress maybe necessary when the damage contributions are not dominated by a single loading source.

Once a master crack growth rate curve exists, the curve can be used to integrate the crack growth rate curve at a specific location to produce a crack growth life curve. [Figure 9.3.11](#) highlights the elements of the analysis.

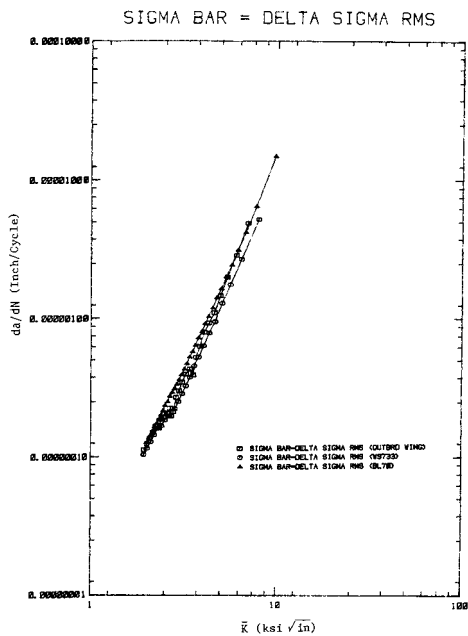


Figure 9.3.10. Cyclic Crack Growth Rate Behavior for Three Transport Wing Stress Histories

$$\bar{K} = \Delta\sigma_{RMS} \cdot (K / \sigma)$$

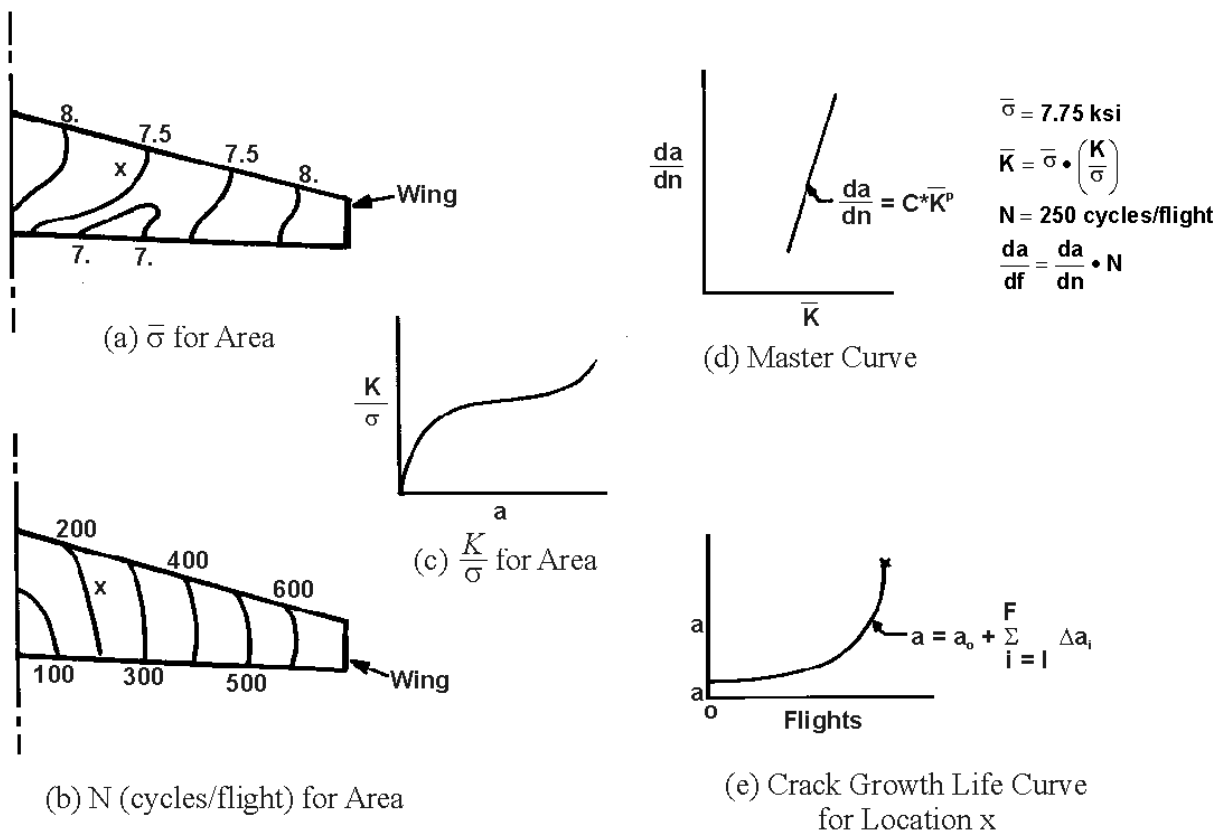


Figure 9.3.11. Schematic of Elements Required to Analyze for Crack Growth Life at Specific Locations